Nanoscale Advances

ROYAL SOCIETY OF CHEMISTRY

PAPER

View Article Online
View Journal | View Issue

Cite this: *Nanoscale Adv.*, 2021, **3**, 4492

Improved performance of lithium–sulfur batteries by employing a sulfonated carbon nanoparticle-modified glass fiber separator

Srikanth Ponnada, *[a] Maryam Sadat Kiai, *[b] Demudu Babu Gorle [c] and Annapurna Nowduri [a]

Some of the most promising alternatives in the energy storage sector are lithium–sulfur batteries, which have a high energy density and theoretical capacity. However, the low electrical conductivity of sulfur and the shuttle effect of polysulfides remain important technical obstacles in the practical use of lithium–sulfur batteries (LSBs). This work employed a glass fiber separator with sulfonated carbon nanoparticles (SCNPs) to reduce the shuttle effect. The negatively charged sulfonic groups in SCNPs might prevent polysulfide migration and anchor lithium polysulfides. By using carbon-based interlayers, this method improves ion conductivity. Furthermore, the equally scattered sulfonic groups serve as active sites, causing sulfur to be distributed consistently and limiting sulfur growth while enhancing active sulfur utilization. After 200 cycles at 1C, the SCNP separator-containing cell showed a specific capacity of 1080 mA h g^{-1}. After 200 cycles, the cell with a CNP separator only showed a specific capacity of 854 mA h g^{-1}, demonstrating that CNPs' polysulfide diffusion suppression was ineffective. The cell with the SCNP separator still showed a high capacity of 901 mA h g^{-1} after 500 cycles, with an average coulombic efficiency of almost 98%.

Received 31st May 2021
Accepted 11th June 2021

DOI: 10.1039/d1na00409c

rsc.li/nanoscale-advances

1. Introduction

Lithium-ion (Li-ion) batteries have revolutionized the portable electronic product market due to their high voltage and energy densities, but going beyond Li-ion batteries to increase battery capacity is essential. The lithium–sulfur (Li–S) cell is one example of electrode materials with alternative electrochemical couples. Li–S cells deliver a specific energy of 2500 W h kg^{-1}, which is roughly three times higher than that of lithium-ion cells (700 W h kg^{-1}), and have sparked a lot of research interest in recent decades.[1–3] One of the most important drawbacks of Li–S batteries is their low rechargeability, which is caused by high solubility of partially reduced sulfur species known as the shuttle effect (LiPS shuttle). The diffusion of soluble LiPS away from the cathode while charging, as well as their unwanted reduction on the anode, leads to reduced coulombic efficiency and fast self-discharge rates for Li–S cells.[4–6,42] Various methods have been used to reduce the shuttle effect in the past, such as modifying the sulfur cathode, separator, electrolyte, or lithium metal anode.[7–11] Many recent studies have focused on keeping polysulfides contained inside the cathode or separator by introducing a chemical or physical barrier.[12–14] The separator in Li–S cells allows lithium ions to pass through, while blocking the diffusion of other ions, particularly polysulfides. Recently, modifying commercial separators with functionalized membrane coatings (carbon compounds, metal oxides, conducting polymers and 2D nanomaterials) has accrued a great deal of interest.[15–18]

Carbon materials including graphene, carbon nanotubes, conductive carbon black, and nano carbon have all been shown to be efficient interlayers in Li–S systems. A carbon interlayer with micropores can serve as a physical barrier, preventing LIPSs from dissolving into the electrolyte through physical or chemical adsorption. Carbon matrixes with a polar composition are typically considered as promising interlayer candidates for the successful entrapment of soluble LIPSs to achieve high specific capacity.[19–22] Most of the carbon matrixes are nonpolar and offer weak interaction with polar Li_2S_X. Cation selection membranes are being used in Li–S batteries. Zhang *et al.* found that using a GO and Nafion membrane with cation selective groups as a blocking layer could greatly reduce the shuttle effect's impact.[23,24] Electron-rich ion selective groups, such as carboxyl and sulfonic groups, have a strong tendency to attract polar Li_2S_X. Most cation selection membranes have low conductivity, resulting in an increase in internal impedance and reduced reutilization of anchored Li_2S_X on the membranes.[25]

[a]*Department of Engineering Chemistry, Andhra University College of Engineering (A), Andhra University, Visakhapatnam-530003, India. E-mail: koolsreekanth@gmail.com*
[b]*Nano-Science and Nano-Engineering Program, Graduate School of Science, Engineering and Technology, Istanbul Technical University, Istanbul 34469, Turkey. E-mail: maryamskiai@gmail.com*
[c]*Materials Research Centre, Indian Institute of Science, Bangalore-560012, India*

Polymers with negatively charged polar groups, such as $-SO_3$ and –COO, can effectively hinder the migration of soluble polysulfides, with the negatively charged groups on cation-selective membranes providing transport channels for Li and thus improving the electrochemical efficiency of Li–S cells. The presence of negatively charged groups allows Li^+ hopping and inhibits the migration of negatively charged polysulfide anions.[26–29]

Many studies have investigated effective methods for immobilizing lithium polysulfides through chemical binding *via* heteroatom doping (such as S, O, and N). Heteroatom doping can improve carbon material conductivity, enhance the affinity between intermediate polysulfides and functionalized carbon frameworks, and improve polysulfide immobilization, all of which improve the electrochemical efficiency of LSBs.[30–32] With the above issues in mind, we employed sulfonated carbon nanoparticles (SCNPs) as a high-efficiency coating on a glass fiber separator to merge ion selective blocking and polar interaction. To accomplish this, we modified electron conductive carbon nanoparticles with sulfonic groups. The SCNPs were coated on a glass fiber separator by using the slurry method. After these modification processes, our cells exhibited high reversible discharge capacities of 1490, 1383, 1249 and 1172 mA h g^{-1} at rates of 1, 2, 4 and 5C, respectively. The rate capability of the cell with the SCNP separator is obviously better than that of the cell with the CNP separator. After 500 cycles at 1C, the cell with the SCNP separator delivered a high capacity of 901 mA h g^{-1}, with an average coulombic efficiency of more than 98%.

2. Experimental section

2.1 Materials

Carbon nanoparticles (<100 nm particle size (TEM), Sigma-Aldrich), sulfuric acid (H_2SO_4 99.999%, Sigma-Aldrich), dimethyl sulfoxide ($(CH_3)_2SO$, anhydrous, ≥99.9%, Sigma-Aldrich), polycarboxylate functionalized graphene (PC-FGF, Sigma-Aldrich), *N*-methyl-2-pyrrolidone (NMP, 99%, Sigma-Aldrich), polyvinylidene fluoride (PVDF, M_w 1000–1200 kg mol^{-1}, Solef 5130, Solvay), 1,3-dioxolane (DOL, 99%, Sigma-Aldrich), 1,2-dimethoxyethane (DME, 99.5%, Sigma-Aldrich), sulfur (S, 99.5–100.5%, Sigma-Aldrich), bis(trifluoromethane) sulfonamide lithium (LiTFSI, 99.95% trace metals basis, Sigma-Aldrich), and lithium nitrate ($LiNO_3$, 99.99%, trace metal basis, Sigma-Aldrich) were used without further purification. The coating was done on glass microfiber filters (Whatman, Grade GF/C) with a thickness of 260 μm.

2.2 Separator preparation (SCNP)

In this study, sulfonated carbon nanoparticles (SCNPs) have been investigated as an efficient coating on a glass fiber separator. The sulfonated glass fiber separator on the face of a cathode allows hopping of positively charged Li ions, but it prevents polysulfide anions from being transported. As a result, it contributes to increased cycling life and capacity retention by suppressing the shuttle of polysulfides between the cathode and anode. These approaches enhanced the ion conductivity by employing carbon based interlayers. Sulfonated carbon nanoparticles cathode facing side glass fiber separator was made using the slurry method, which involved combining 210 mg of the treated sulfonated carbon composite and 60 mg of dimethyl sulfoxide ($(CH_3)_2SO$) in a 2.33 ml PVDF-NMP solution. The slurry was cast onto one side of a glass fiber separator and vacuum dried at 60 °C for 24 h. For treated sulfonated carbon composite preparation, first 10 mg of nano carbon were put inside the glass fiber separator and then put into a mixture of 5 ml H_2SO_4 and 100 ml dimethyl sulfoxide and stirred at 80 °C for 4 h, and then the carbon composite was filtered, washed with deionized water and finally dried in a vacuum oven at 60 °C for 24 h (Scheme 1).

In this method, subjecting the nano carbon to concentrated sulfuric acid (H_2SO_4) was investigated with high sulfonic acid loadings (>1 mmol g^{-1}), to alleviate the unwanted oxidation of the carbon substrate by SO_3 and/or H_2SO_4, and nano carbon was sealed into a separator pouch.

2.3 Cathode preparation

The sulfur cathode was prepared using the slurry technique. First, polycarboxylate functionalized graphene (PC-FGF) and sulfur powder were combined in *N*-methyl-2-pyrrolidone at a weight ratio of 80 wt% S, 10 wt% PC-FGF, and 10% NMP (12 wt% PVDF in NMP) and ground in an agate mortar to produce a slurry, which was then coated onto aluminum foil using the doctor blade method. The coated cathode was dried for 12 hours in an air oven at 60 °C and cut into 12 mm disks. The S loading in was 5 mg cm^{-2}.

2.4 Electrolyte preparation

1 M bis(trifluoromethane) sulfonamide lithium (LiTFSI) in a solvent mixture of 1,3-dioxolane (DOL) and 1,2-dimethoxyethane (DME) (1 : 1) was considered as an efficient electrolyte for polysulfide trapping. The amount of electrolyte in each coin cell was kept constant at 20 L mg^{-1} of S.

2.5 Characterization

CR2032-type coin cells were assembled with the PC-FGF/S composite cathode, CNP and SCNP coated glass fiber separators, lithium metal anode and electrolyte in an argon-filled glove box. The cells were cycled between 1.4 and 3.2 V on a Neware BTS 3008 battery tester. Surface characterization of the modified separators was carried out using SEM equipped with an EDS. Cyclic voltammetry (CV) measurements and electrochemical impedance spectroscopy (EIS) tests were performed using a CHI660E electrochemical workstation at a scan rate of 0.1 mV s^{-1} in the potential range of 3.2–1.4 V (*vs.* Li^+/Li) and 1 MHz to 1 Hz at an AC voltage amplitude of 10 mV. XRD diffraction analysis was carried out with a Rigaku SmartLab diffractometer by using filter Cu Kα radiation (k = 1.541 Å). Raman analysis was carried out with a Renishaw Raman Spectroscopy system using a 532 nm argon laser as the excitation source. Elemental compositions were analyzed using X-ray

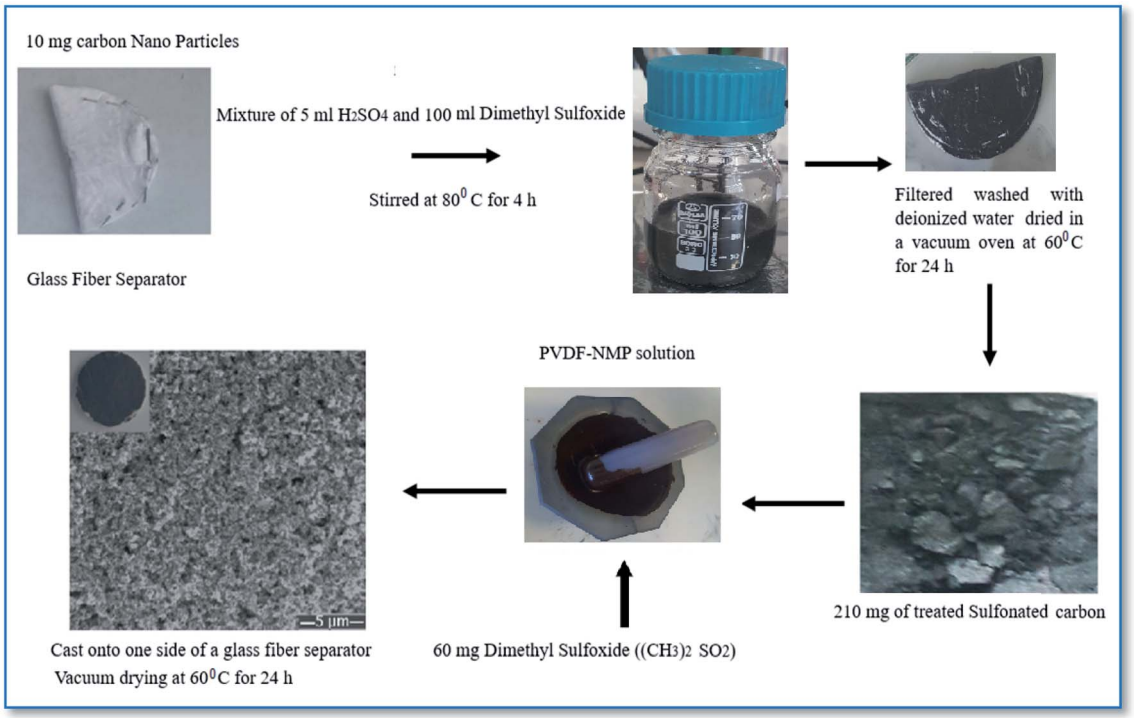

Scheme 1 Synthesis of sulfonated carbon nanoparticles on a glass fiber separator.

photoelectron spectroscopy (hemispherical analyzer, Thermo Scientific K-Alpha XPS).

3. Results and discussion

Fig. 1 shows the SEM images and elemental mapping analysis of CNPs, and CNP and SCNP separators. The coating thickness on the glass fiber separator was approximately 35 µm. The carbon nanoparticle- and sulfonated carbon nanoparticle-coated separators can be seen in the SEM photographs shown in Fig. 1b and c. They have flat plate morphologies and they are tightly attached to the glass fiber separators. The SCNP layer is more porous, which may make it easier to capture the soluble polysulfides.

Fig. 1d–i display the corresponding EDS elemental mapping for carbon, oxygen, and sulfur, respectively. The sulfonic groups are evenly distributed on the SCNP surfaces, employing carbon and oxygen as references.

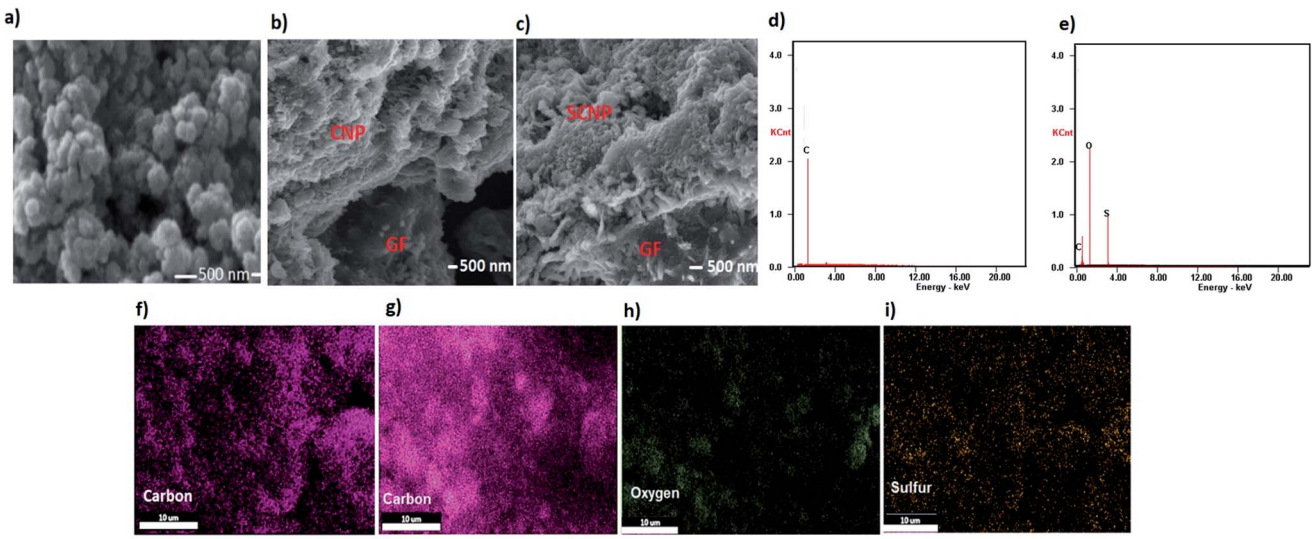

Fig. 1 FE- SEM images of (a) carbon nanoparticles (b) carbon nanoparticles on glass fiber surface (c) sulfonated carbon nanoparticles on glass fiber surface; EDS elemental of (d) carbon nanoparticles (e) sulfonated carbon nanoparticles mapping of (f) carbon corresponding to (b); (g) carbon (h) oxygen, and (i) sulfur corresponding to (c).

As shown in Fig. 2a, CNP Raman peaks are located at 1252 and 1753 cm^{-1} (ν C=C). After sulfonation, a peak at 1256 (C=C) and a shifted peak at 1690 cm^{-1} (ν S–O) are observed corresponding to the stretching bands of the sulfonic acid groups, proving the successful introduction of sulfonic groups on the CNPs.

The XPS survey spectra of CNP and SCNP separators are shown in Fig. 2b. O 1s, C 1s, S 2s and S 2p peaks were observed at 527, 338, 246 and 172 eV, respectively. The XPS spectrum specifically reveals that the SCNPs incorporate sulfonic groups. The S 2p XPS spectrum (Fig. 2c) displays two main peaks at 164.9 and 172.1 eV, which could be assigned to S $2p_{1/2}$ and S $2p_{3/2}$, respectively.[33,34]

As seen in Fig. 3a, the cell with the SCNP separator showed a specific capacity of 1080 mA h g^{-1} after 200 cycles at 1C (1C = 1675 mA g^{-1}). In contrast, the cell with a CNP separator displayed a specific capacity of only 854 mA h g^{-1} after 200 cycles, indicating that CNPs' suppression of polysulfide diffusion was much less effective. The rate capability of the cells is shown in Fig. 3b. The cell with the SCNP separator demonstrates specific capacities of 1490, 1383, 1249 and 1172 mA h g^{-1} at rates of 1, 2, 4 and 5C, respectively. When it returns to 2C after 50 cycles, the

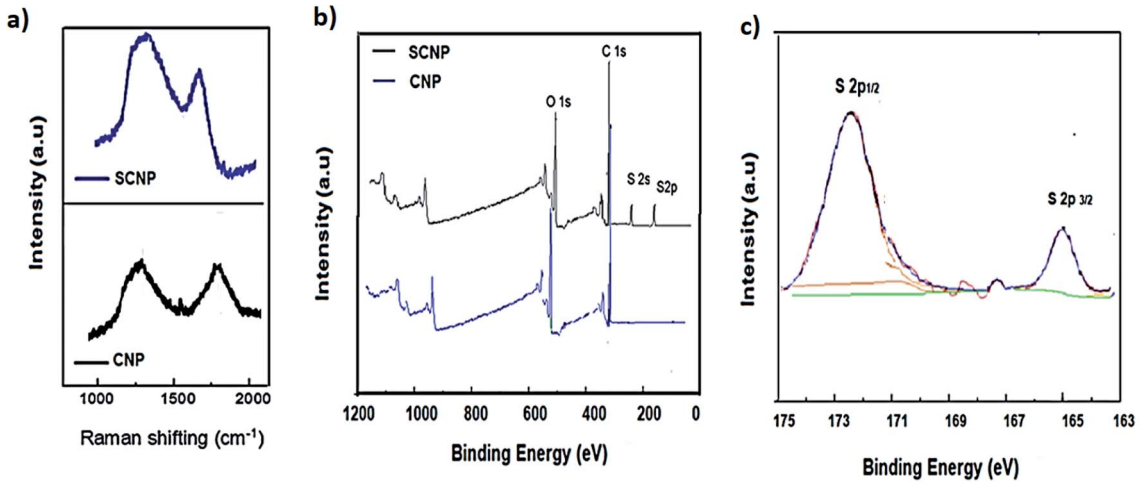

Fig. 2 (a) Raman spectra of CNPs and SCNPs. (b) XPS spectra of CNPs and SCNPs; (c) corresponding high-resolution S 2p XPS spectrum of SCNPs.

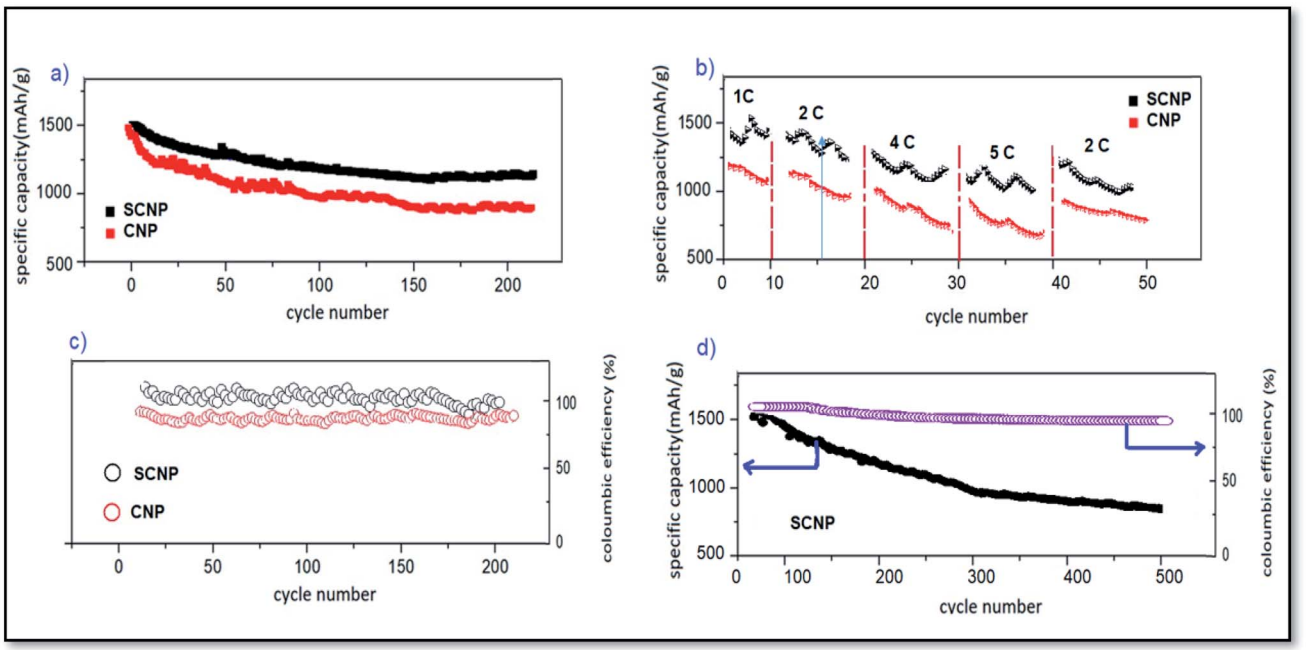

Fig. 3 (a) Cycling performance, (b) rate performance and (c) coulombic efficiency of the cells with CNP and SCNP separators at 1C. (d) Long-term cycling performance of the cell with the SCNP separator at the rate of 1C.

discharge capacity recovers to 1247 mA h g^{-1}. The rate capability of the cell with the SCNP separator is obviously better than that of the cell with the CNP separator. The cell with SCNPs delivered a higher average coulombic efficiency of 100% after 200 cycles at a rate of 1C. In contrast, the coulombic efficiency of the cell with the CNP separator decreased up to 85% after 200 cycles, indicating less suppression of polysulfide diffusion by CNPs (Fig. 3c).

Long-term cycling stability was investigated for the cell with the SCNP separator and is shown in Fig. 3d. After 500 cycles at 1C, the cell with the SCNP separator delivered a high capacity of 901 mA h g^{-1}, with an average coulombic efficiency of more than 98%.

Fig. 4a shows the CV curves of the cells with CNP and SCNP separators at a scan rate of 0.1 mV s^{-1}. The cell with the SCNP separator exhibits two sharp cathodic peaks located at 2.40 V and 1.80 V where the peaks are related to the conversion of sulfur to the long chain polysulfides (S_X^{2-}, $4 < X \leq 8$) and subsequently reduction to short chain polysulfides (Li_2S_2 and Li_2S). One sharp anodic peak is located at 2.42 V corresponding

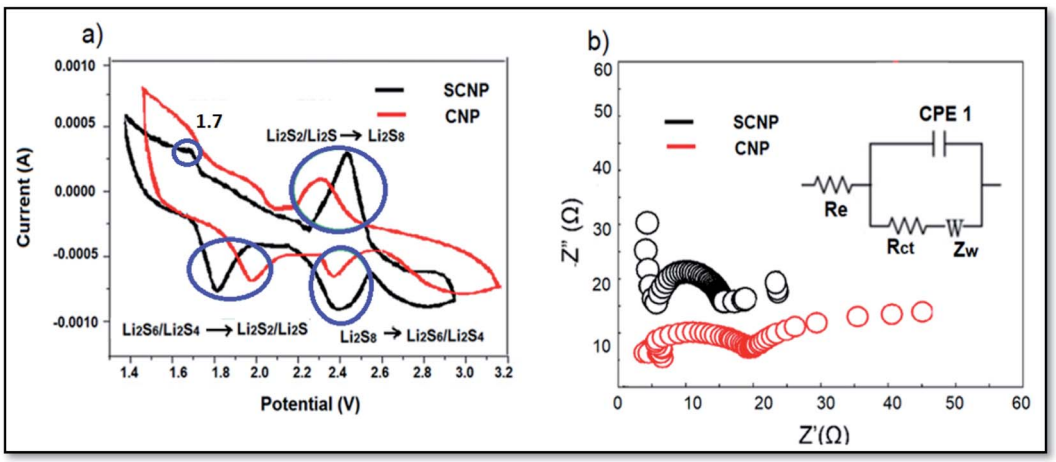

Fig. 4 (a) Cyclic voltammetry (CV) curves of the cells with CNP and SCNP separators at a scan rate of 0.1 mV s^{-1} and in the voltage range from 1.4 to 3.0 V. (b) Impedance spectra of the fresh cells with CNP and SCNP separators.

Table 1 Fitted values for the equivalent circuit elements

Separators	CNPs	SCNPs
R_e (Ω)	0.430	0.541
R_{ct} (Ω)	16.2	20.1
CPE (F)	1.092×10^{-7}	0.696×10^{-7}
Z_w (S. sec^.5)	0.0038	0.0041

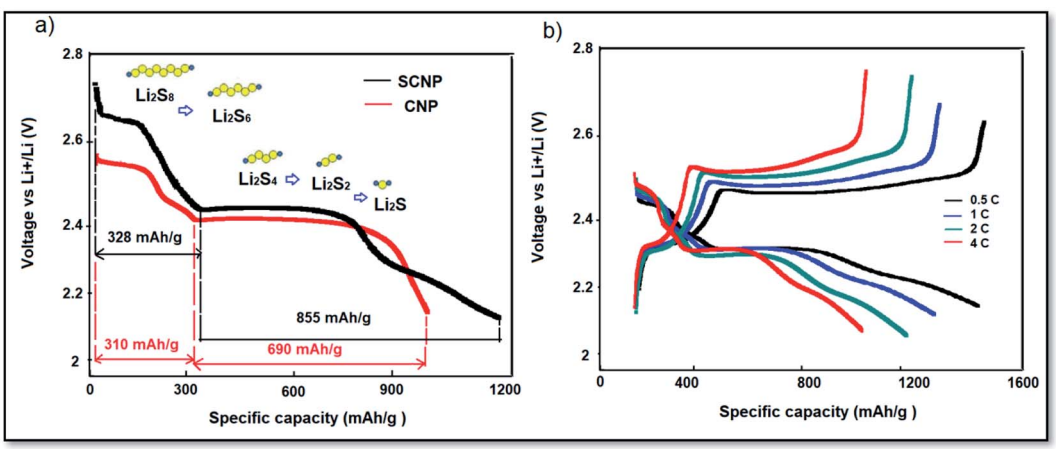

Fig. 5 (a) The hundredth discharge curves of the cells with CNPs and SCNPs; (b) the discharge curves of the cell with SCNPs at different current rates between 2.8 and 2 V *vs.* Li^+/Li.

to the oxidation process of short chain polysulfides to long chain polysulfides and original sulfur. For the cell containing SCNPs, a very weak oxidation peak at about 1.7 V is seen, which may be attributed to Li^+ extraction from SCNPs. The cathodic scan, however, shows no corresponding reduction peak (Li^+ insertion into SCNPs), which may be explained by the cathodic peak, 1.80 V, being extremely near the potential of Li^+ insertion into SCNPs.[35,36]

The cell with the CNP separator showed a shift in cathodic peaks to 2.38 V and 1.98 V. The broad anodic one is located at 2.30 V. In comparison to the case of CNPs, the CV curve of the cell with SCNPs showed higher current intensity and a greater redox field indicating a more reversible redox reaction. An EIS impedance test was performed for both cells.

As shown in Fig. 4b, the fresh cell with the SCNP separator demonstrates lower impedance displaying higher polysulfide trapping ability of SCNPs than that of CNPs. Table 1 displays the fitted values. The ohmic resistance R_e for both batteries is about 4 Ω meaning that both cells were correctly fabricated and tested in the same state. It can also be shown that the charge transfer resistance (R_{ct}) of the cell using CNPs is much higher than the charge transfer resistance (R_{ct}) of the cell using SCNPs. The

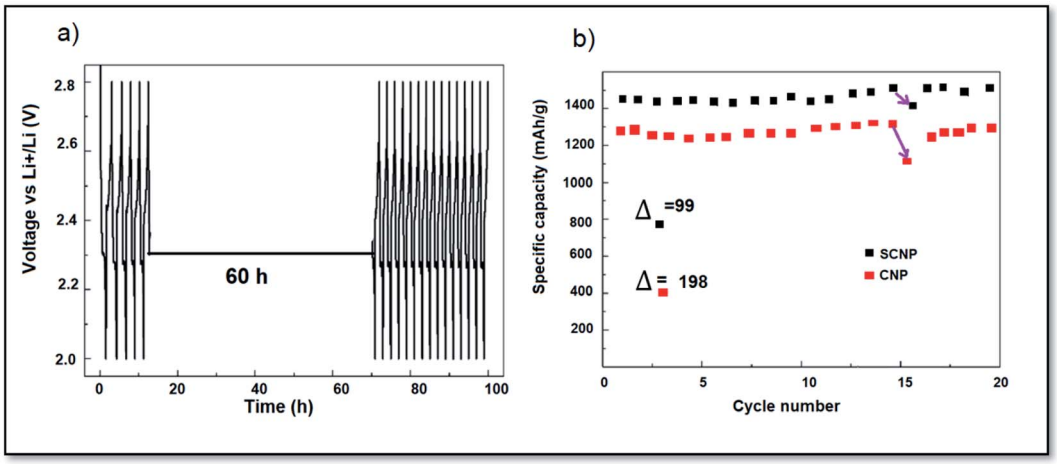

Fig. 6 (a) Time–voltage curve of the interruption process (the sixteenth discharge was suspended at 2.3 V for 60 h) and (b) the corresponding performance.

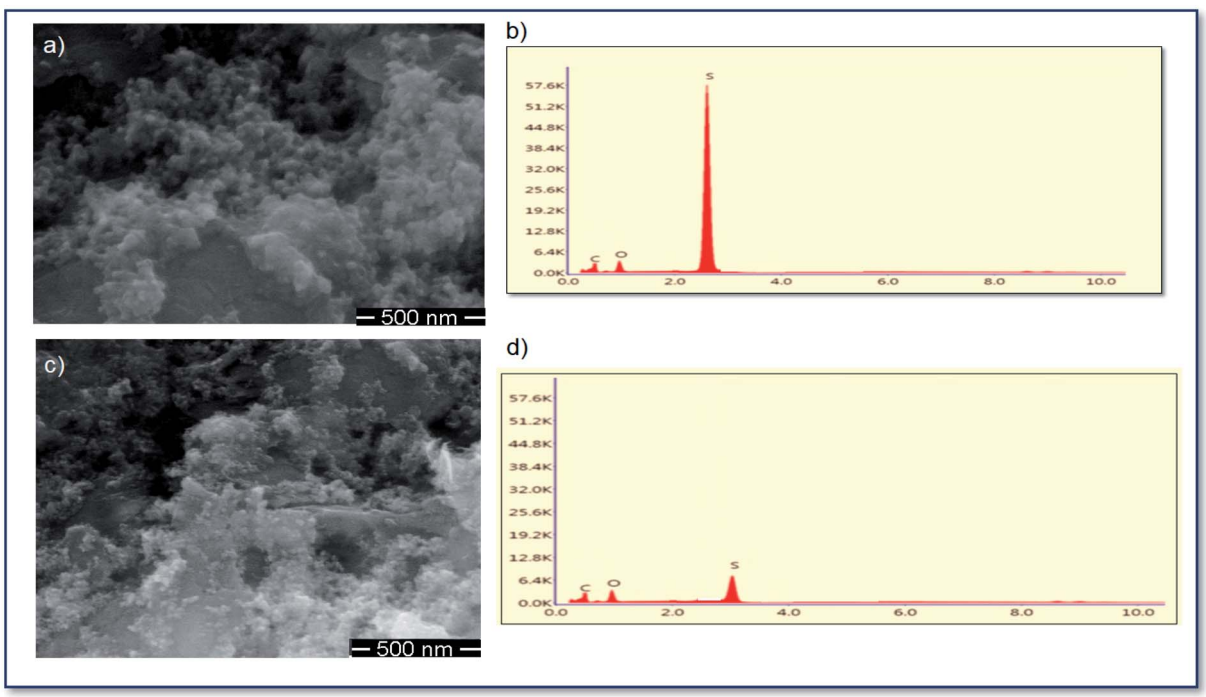

Fig. 7 SEM images of the surface views of (a) SCNP and (c) CNP separators for 200 cycles at 1C, and the corresponding EDS analysis of (b) SCNPs and (d) CNPs.

addition of sulfonic groups efficiently minimized the R_{ct} from 20.1 for the cell with CNPs to 16.2 Ω for the cell with SCNPs, resulting in lower cell polarization.

The hundredth discharge curves of the cells with CNP and SCNP separators are shown in Fig. 5a. The cell with the SCNP separator demonstrated a discharge capacity of 1183 mA h g^{-1}, with two discharge plateaus at 328 and 855 mA h g^{-1}, respectively. The discharge capacities related to the two plateaus of the cell with SCNPs are larger, reflecting that the incorporation of sulfonic groups leads to higher utilization of soluble polysulfides and more efficient conversion and reduction of polysulfides. On the other hand, the CNPs could only serve as a physical shield for the polysulfides.[37,38] The rate capability of the cell with SCNPs has been investigated under various C rates from 0.5 to 4C as shown in Fig. 5b. The uniformly distributed sulfonic groups could contribute to a uniform polysulfide distribution. Consequently, the excessive aggregation of lithium sulfides may be alleviated to some degree in the subsequent discharge process. As a result, the cyclability of the cell with SCNPs under different rates delivers 1470, 1307, 1202 and 1038 mA h g^{-1} at 0.5C, 1C, 2C and 4C rates, respectively, indicating the advantages of the sulfonic groups in increasing the electrochemical performance of the cell even at a high rate of current.

The efficiency of self-discharge was evaluated and the discharge was suspended at 2.3 V for 60 hours at the sixteenth discharge.[39,40] The soluble polysulfides can move to the lithium anode during the interruption, resulting in the lack of active content. The capacity failure of self-discharge is represented by $\Delta/Q_{sixteenth}$. The Δ values of CNPs and SCNPs were 198 and 99 mA h g^{-1}, corresponding to a loss rate of 18.1%, and 7.2%, respectively. The cell with SCNPs exhibits superior inhibition of self-discharge (Fig. 6).

Fig. 7a–c show the SEM images and EDS analysis of SCNP separator surfaces cycled for 200 cycles at 1C. In comparison to that before cycling, the cell with SCNPs showed more polysulfide adsorption on the separator surface after 200 cycles, showing that the sulfonic groups can effectively adsorb polysulfides. The stronger sulfur signal in the SCNP surface means less polysulfide migration toward the anode and the SCNP coatings on the separator can alleviate the migration of polysulfides as well. As shown in Fig. 7b–d, the sulfur signal was lower, proving that more polysulfides migrate toward the anode, leading to severe capacity fading.

The XPS S 2p spectra of the CNPs and SCNPs are measured before and after cycling in order to better understand polysulfide blocking and adsorption. All samples are completely washed with

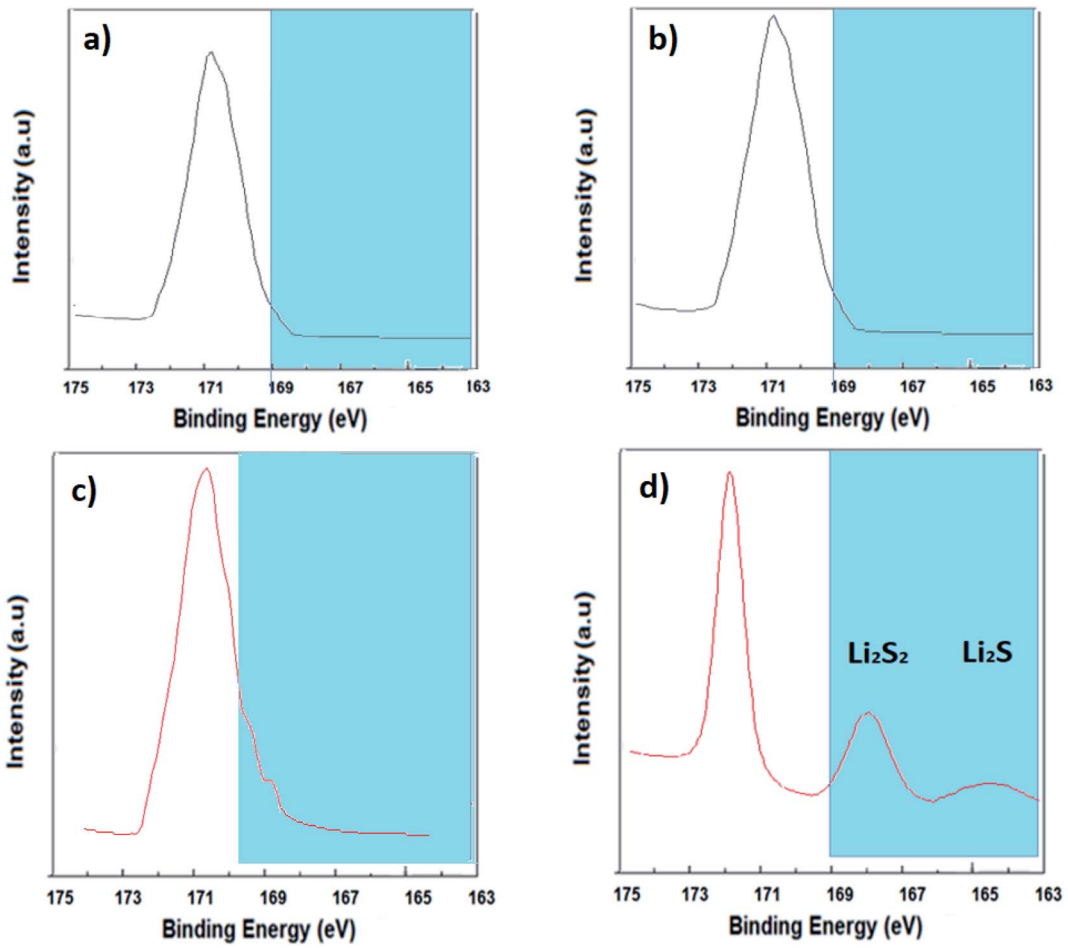

Fig. 8 Raw XPS spectra of (a) fresh CNPs, (b) CNPs after cycling, (c) fresh SCNPs and (d) SCNPs after cycling.

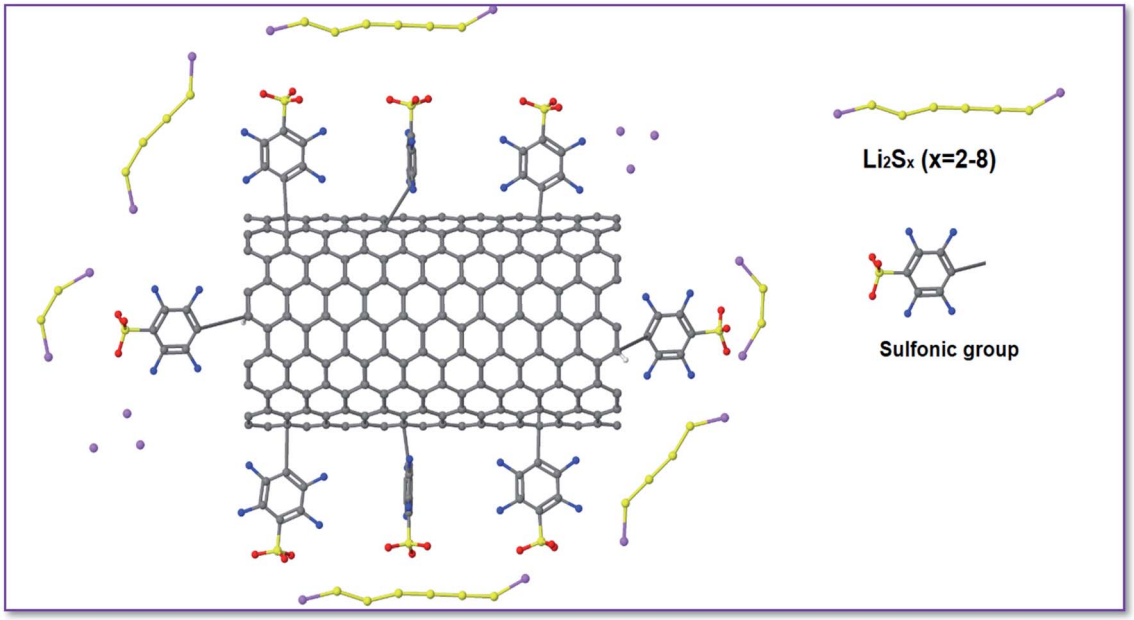

Fig. 9 Representation of the electro-chemical interaction of sulfonic and lithium sulfides on carbon particles. Red, yellow, gray, white, blue and purple indicate oxygen (O), sulphur (S), carbon (C), hydrogen (H), nitrogen (N) and lithium (Li), respectively.

DME prior to XPS testing. Fig. 8a and b show no obvious peaks for Li_2S–S and Li_2S_2–S molecules. In contrast, the Li_2S–S and Li_2S_2–S molecules were clearly observed on the surface of SCNPs after cycling (binding energies of 168 and 164.5 eV). The XPS spectra which support polysulfides adsorption on SCNPs are shown in Fig. 8c and d. As a result, the adsorption of polysulfides on the surface of SCNPs has been thoroughly established.[41]

As shown in Fig. 9, we combined ion selective blocking and polar contact to create a high-efficiency interlayer. The electron conductive CNPs were modified with sulfonic groups and a chemical process was used to introduce the SCNPs onto the glass fiber separator.

4. Conclusion

Cycling stability, rate capability, coulombic performance, and self-discharge inhibition in the cell are all improved by the presence of sulfonic groups on CNPs as a dual functional glass fiber. The SCNP-treated cell has a higher level of self-discharge inhibition. The cyclability of the cell with SCNPs at various rates yields 1470, 1307, 1202 and 1038 mA h g^{-1} at 0.5C, 1C, 2C, and 4C rates, respectively, demonstrating the benefits of the sulfonic groups in improving the electrochemical performance of the cell even at high current rates. The CV curve of the cell with SCNPs showed a higher current intensity and a larger redox field than the CV curve of the cell with CNPs, suggesting a more reversible redox reaction. Unlike complicated separator or cathode preparation, our work is easy to experiment with and reproduce, making it perfect for practical use and scale-up production.

Conflicts of interest

There are no conflicts to declare.

Acknowledgements

Dr Maryam Sadat Kiai would like to thank Istanbul Technical University, Istanbul. Also, we would like to thank Andhra University College of Engineering, Andhra University, Visakhapatnam-India, and IISC-Bangalore-India, for resource support. Srikanth Ponnada and Dr Annapurna Nowduri would like to thank Andhra University College of Engineering, Andhra University, Visakhapatnam-India; Indian Institute of Science-Bangalore; Istanbul Technical University, Istanbul-Turkey for resource and technical support and also grateful to University Grants Commission-Govt of India. Dr Demudu Babu Gorle would like to thank the Indian Institute of Science Bangalore; University Grants Commission and Government of India for providing Dr D. S. Kothari a Postdoctoral Fellowship; Andhra University College of Engineering, Andhra University, Visakhapatnam, India; and Istanbul Technical University-Turkey.

References

1 *Handbook of Battery Materials*, ed. C. Daniel and J. O. Besenhard, John Wiley & Sons, 2012.
2 P. G. Bruce, S. A. Freunberger, L. J. Hardwick and J. M. Tarascon, Li–O 2 and Li–S batteries with high energy storage, *Nat. Mater.*, 2012, **11**(1), 19–29.
3 M. Jana, R. Xu, X. B. Cheng, J. S. Yeon, J. M. Park, J. Q. Huang, Q. Zhang and H. S. Park, Rational design of two-dimensional nanomaterials for lithium–sulfur batteries, *Energy Environ. Sci.*, 2020, **13**(4), 1049–1075.
4 H. S. Ryu, H. J. Ahn, K. W. Kim, J. H. Ahn, K. K. Cho and T. H. Nam, Self-discharge characteristics of lithium/sulfur batteries using TEGDME liquid electrolyte, *Electrochim. Acta*, 2006, **52**(4), 1563–1566.

5 M. Barghamadi, A. S. Best, A. I. Bhatt, A. F. Hollenkamp, M. Musameh, R. J. Rees and T. Rüther, *Energy Environ. Sci.*, 2014, **7**, 3902–3920.
6 Q. Wang, J. Jin, X. Wu, G. Ma, J. Yang and Z. Wen, A shuttle effect free lithium sulfur battery based on a hybrid electrolyte, *Phys. Chem. Chem. Phys.*, 2014, **16**(39), 21225–21229.
7 A. Eftekhari and D. W. Kim, Cathode materials for lithium–sulfur batteries: a practical perspective, *J. Mater. Chem. A*, 2017, **5**(34), 17734–17776.
8 Y. He, Y. Qiao and H. Zhou, Recent advances in functional modification of separators in lithium–sulfur batteries, *Dalton Trans.*, 2018, **47**(20), 6881–6887.
9 A. Gupta, A. Bhargav and A. Manthiram, Highly solvating electrolytes for lithium–sulfur batteries, *Adv. Energy Mater.*, 2019, **9**(6), 1803096.
10 T. Tao, S. Lu, Y. Fan, W. Lei, S. Huang and Y. Chen, Anode improvement in rechargeable lithium–sulfur batteries, *Adv. Mater.*, 2017, **29**(48), 1700542.
11 R. Kumar, J. Liu, J. Y. Hwang and Y. K. Sun, Recent research trends in Li–S batteries, *J. Mater. Chem. A*, 2018, **6**(25), 11582–11605.
12 W. Fan, L. Zhang and T. Liu, Multifunctional second barrier layers for lithium–sulfur batteries, *Mater. Chem. Front.*, 2018, **2**(2), 235–252.
13 Y. C. Jeong, J. H. Kim, S. Nam, C. R. Park and S. J. Yang, Rational design of nanostructured functional interlayer/separator for advanced Li–S batteries, *Adv. Funct. Mater.*, 2018, **28**(38), 1707411.
14 S. A. Abbas, J. Ding, S. H. Wu, J. Fang, K. M. Boopathi, A. Mohapatra, L. W. Lee, P. C. Wang, C. C. Chang and C. W. Chu, Modified separator performing dual physical/chemical roles to inhibit polysulfide shuttle resulting in ultrastable Li–S batteries, *ACS Nano*, 2017, **11**(12), 12436–12445.
15 S. A. Abbas, M. A. Ibrahem, L. H. Hu, C. N. Lin, J. Fang, K. M. Boopathi, P. C. Wang, L. J. Li and C. W. Chu, Bifunctional separator as a polysulfide mediator for highly stable Li–S batteries, *J. Mater. Chem. A*, 2016, **4**(24), 9661–9669.
16 Y. He, Z. Chang, S. Wu and H. Zhou, Effective strategies for long-cycle life lithium–sulfur batteries, *J. Mater. Chem. A*, 2018, **6**(15), 6155–6182.
17 M. Rana, M. Li, X. Huang, B. Luo, I. Gentle and R. Knibbe, Recent advances in separators to mitigate technical challenges associated with re-chargeable lithium sulfur batteries, *J. Mater. Chem. A*, 2019, **7**(12), 6596–6615.
18 J. Ci, C. Cao, S. Kuga, J. Shen, M. Wu and Y. Huang, Improved performance of microbial fuel cell using esterified corncob cellulose nanofibers to fabricate air-cathode gas diffusion layer, *ACS Sustainable Chem. Eng.*, 2017, **5**(11), 9614–9618.
19 R. Singhal, S. H. Chung, A. Manthiram and V. Kalra, A free-standing carbon nanofiber interlayer for high-performance lithium–sulfur batteries, *J. Mater. Chem. A*, 2015, **3**(8), 4530–4538.
20 C. H. Chang, S. H. Chung and A. Manthiram, Effective stabilization of a high-loading sulfur cathode and a lithium-metal anode in Li-S batteries utilizing SWCNT-modulated separators, *Small*, 2016, **12**(2), 174–179.
21 J. Balach, T. Jaumann, M. Klose, S. Oswald, J. Eckert and L. Giebeler, Improved cycling stability of lithium–sulfur batteries using a polypropylene-supported nitrogen-doped mesoporous carbon hybrid separator as polysulfide adsorbent, *J. Power Sources*, 2016, **303**, 317–324.
22 J. Zhu, Y. Ge, D. Kim, Y. Lu, C. Chen, M. Jiang and X. Zhang, A novel separator coated by carbon for achieving exceptional high-performance lithium-sulfur batteries, *Nano Energy*, 2016, **20**, 176–184.
23 J. Q. Huang, T. Z. Zhuang, Q. Zhang, H. J. Peng, C. M. Chen and F. Wei, Permselective graphene oxide membrane for highly stable and anti-self-discharge lithium–sulfur batteries, *ACS Nano*, 2015, **9**(3), 3002–3011.
24 J. Q. Huang, Q. Zhang, H. J. Peng, X. Y. Liu, W. Z. Qian and F. Wei, Ionic shield for polysulfides towards highly-stable lithium–sulfur batteries, *Energy Environ. Sci.*, 2014, **7**(1), 347–353.
25 T. Z. Hou, X. Chen, H. J. Peng, J. Q. Huang, B. Q. Li, Q. Zhang and B. Li, Design principles for heteroatom-doped nanocarbon to achieve strong anchoring of polysulfides for lithium–sulfur batteries, *Small*, 2016, **12**(24), 3283–3291.
26 K. Yang, L. Zhong, Y. Mo, R. Wen, M. Xiao, D. Han, S. Wang and Y. Meng, A functional separator coated with sulfonated poly (styrene-ethylene-butylene-styrene) to synergistically enhance the electrochemical performance and anti-self-discharge behavior of Li–S batteries, *ACS Appl. Energy Mater.*, 2018, **1**(6), 2555–2564.
27 X. Luo, X. Lu, G. Zhou, X. Zhao, Y. Ouyang, X. Zhu, Y. E. Miao and T. Liu, Ion-selective polyamide acid nanofiber separators for high-rate and stable lithium–sulfur batteries, *ACS Appl. Mater. Interfaces*, 2018, **10**(49), 42198–42206.
28 D. B. Babu, K. Giribabu and K. Ramesha, Permselective SPEEK/Nafion composite-coated separator as a potential polysulfide crossover barrier layer for Li–S batteries, *ACS Appl. Mater. Interfaces*, 2018, **10**(23), 19721–19729.
29 K. Jiang, S. Gao, R. Wang, M. Jiang, J. Han, T. Gu, M. Liu, S. Cheng and K. Wang, Lithium sulfonate/carboxylate-anchored polyvinyl alcohol separators for lithium sulfur batteries, *ACS Appl. Mater. Interfaces*, 2018, **10**(21), 18310–18315.
30 J. Yang, F. Chen, C. Li, T. Bai, B. Long and X. Zhou, A free-standing sulfur-doped microporous carbon interlayer derived from luffa sponge for high performance lithium–sulfur batteries, *J. Mater. Chem. A*, 2016, **4**(37), 14324–14333.
31 S. Ponnada, M. S. Kiai, D. B. Gorle and A. Nowduri, Application of facile novel L-GO binder with modified nanocomposite coatings for efficient performance of lithium sulfur battery, *ACS Energy & Fuels*, 2021, accepted.
32 S. Ponnada, M. S. Kiai, D. B. Gorle and A. Nowduri, An Insight into Lithium-Sulphur Batteries with Novel Modified Separators: Recent Progress and Perspectives, *ACS Energy & Fuels*, 2021, DOI: 10.1021/acs.energyfuels.1c01509.

33 L. Zhou, X. Lin, T. Huang and A. Yu, Binder-free phenyl sulfonated graphene/sulfur electrodes with excellent cyclability for lithium sulfur batteries, *J. Mater. Chem. A*, 2014, **2**(14), 5117–5123.

34 Y. Lu, S. Gu, J. Guo, K. Rui, C. Chen, S. Zhang, J. Jin, J. Yang and Z. Wen, Sulfonic groups originated dual-functional interlayer for high performance lithium–sulfur battery, *ACS Appl. Mater. Interfaces*, 2017, **9**(17), 14878–14888.

35 H. Pan, X. Huang, X. Yan, L. Liu, L. Xia and T. Zhang, Metal-doped mesoporous silica as sulfur hosts in lithium-sulfur battery with enhanced conductivity and polysulfide adsorption ability, *J. Electroanal. Chem.*, 2019, **832**, 361–367.

36 Y. Wan, Y. Hong, X. Bei, J. Hao, H. You, C. Niu, H. Yang and X. Liu, Ketjen Black–titanium dioxide coated glass fiber separator for high performance Li/S cells using bare sulfur cathode, *J. Mater. Sci.: Mater. Electron.*, 2019, **30**(7), 7054–7064.

37 Z. Xiao, Z. Yang, L. Wang, H. Nie, M. E. Zhong, Q. Lai, X. Xu, L. Zhang and S. Huang, A lightweight TiO2/graphene interlayer, applied as a highly effective polysulfide absorbent for fast, long-life lithium–sulfur batteries, *Adv. Mater.*, 2015, **27**(18), 2891–2898.

38 Y. Guo, M. Sun, H. Liang, W. Ying, X. Zeng, Y. Ying, S. Zhou, C. Liang, Z. Lin and X. Peng, Blocking polysulfides and facilitating lithium-ion transport: polystyrene sulfonate@HKUST-1 membrane for lithium–sulfur batteries, *ACS Appl. Mater. Interfaces*, 2018, **10**(36), 30451–30459.

39 C. J. Hart, M. Cuisinier, X. Liang, D. Kundu, A. Garsuch and L. F. Nazar, Rational design of sulphur host materials for Li–S batteries: correlating lithium polysulphide adsorptivity and self-discharge capacity loss, *Chem. Commun.*, 2015, **51**(12), 2308–2311.

40 L. Wang, J. Liu, S. Yuan, Y. Wang and Y. Xia, To mitigate self-discharge of lithium–sulfur batteries by optimizing ionic liquid electrolytes, *Energy Environ. Sci.*, 2016, **9**(1), 224–231.

41 S. Xiong, K. Xie, Y. Diao and X. Hong, On the role of polysulfides for a stable solid electrolyte interphase on the lithium anode cycled in lithium–sulfur batteries, *J. Power Sources*, 2013, **236**, 181–187.

42 S. Ponnada, M. S. Kiai, D. B. Gorle and A. Nowduri, History and Recent Developments in Divergent Electrolytes towards High Efficiency of Lithium–Sulfur Battery's–a Review, *Mater. Adv.*, 2021, DOI: 10.1039/d1ma00332a.